Ultrafine Ni–Co–W–B amorphous alloys and their activities in benzene hydrogenation to cyclohexane

Ming-Hua Qiao, Song-Hai Xie, Wei-Lin Dai and Jing-Fa Deng *

Department of Chemistry, Fudan University, Shanghai 200433, PR China
E-mail: jfdeng@srcap.stc.sh.cn

Received 18 July 2000; accepted 15 November 2000

Quaternary Ni–Co–W–B amorphous alloys were prepared by chemical reduction of the aqueous solution of nickel and cobalt salts and sodium tungstate with potassium borohydride. The catalytic activities of the as-prepared materials were measured through liquid phase hydrogenation of benzene under moderate pressure. In comparison with Ni–Co–B, the as-prepared Ni–Co–W–B amorphous alloys showed superior activity, attributable to the promoting effect of tungsten on the microstructure of the alloys as revealed by XPS, XRD and DSC measurements.

KEY WORDS: amorphous alloys; benzene; hydrogenation; Ni–Co–W–B

1. Introduction

Benzene hydrogenation to cyclohexane is of great significance in the viewpoint of the petroleum industry and environment protection. Cyclohexane is the precursor for Nylon-6 and Nylon-66. Phenol and cyclohexylamine can be prepared in the cyclohexane route. On the other hand, the existence of excessive amount of aromatics in kerosene leads to serious air pollution as well. However, because hydrogenation of aromatics is more difficult than hydrodesulfurization (HDS) or hydrodenitrogenation (HDN), the content of aromatics does not decrease in appreciable amount in a routine hydrorefinement process. Kinetic and thermodynamic results also show that polyaromatics are easier to be reduced than benzene under moderate condition [1], thus the development of an active benzene hydrogenation catalyst is highly appreciated.

Recently amorphous metal alloys have gained much attention as promising novel catalytic materials [2]. Their unique isotropic structure and high concentration of coordinatively unsaturated sites [3] lead to superior catalytic activity and selectivity to their crystalline counterparts. In particular, amorphous alloys prepared by chemical reduction using borohydride (BH_4^-) or hypophosphite ($H_2PO_2^-$) bear nanosized morphology and consequently higher surface area and reactivity than those prepared by the quenching method [4]. Furthermore, nanosized particles can readily eliminate inner diffusion and facilitate excellent suspensibility in liquid phase reaction, which is beneficial for sufficient contact with the reactants.

In this paper, we present the preparation and characterization of a series of Ni–Co–W–B amorphous alloys and their activities in benzene hydrogenation to cyclohexane. It is found that these quaternary amorphous alloys exhibit excellent benzene hydrogenation activity. Some important factors that influence the catalytic behavior, such as preparation temperature and the solvents used in hydrogenation, were also explored. The experimental results were correlated with their structural and electronic properties identified by ICP, BET, DSC, XRD, XPS and TEM characterizations.

* To whom correspondence should be addressed.

2. Experimental

2.1. Catalyst preparation

The Ni–Co–W–B particles were prepared by a chemical reduction method described as follows. An aqueous solution of potassium borohydride (KBH_4, 2.00 M) was added dropwise into a mixed aqueous solution of nickel acetate ($Ni(CH_3COO)_2{\cdot}4H_2O$, 0.20 M), cobalt acetate ($Co(CH_3COO)_2{\cdot}4H_2O$, 0.20 M) and sodium tungstate ($Na_2WO_4{\cdot}2H_2O$, 0.20 M) with gentle stirring. The molar ratio of B/(Ni + Co + 3W) was 5/2 with equimolar amount of Ni and Co in the solution. Ni–Co–W–B alloys with different tungsten content were obtained by adjusting the volume of sodium tungstate added. After the fine black precipitates were obtained, they were washed with oxygen-free distilled water and 99.5% ethanol successively before using as hydrogenation catalysts of benzene. During washing, care must be taken to keep the powders from contacting with air.

2.2. Catalyst characterization

The compositions of the Ni–Co–W–B alloys were analyzed by inductively coupled plasma atomic emission spectroscopy (ICP-AES). The specific surface areas (S_{BET}) were measured by physisorption of N_2 at 77 K on Micromeritics ASAP 2000. The morphologies of the alloys were studied by transmission electron microscopy (TEM) on a Hi-

Table 1
Specific surface area, bulk and surface composition of the as-prepared Ni–Co–W–B series alloys.[a]

Sample (Ni : Co : W molar ratio for initial solution)	Bulk composition (atomic ratio)	Surface composition (atomic ratio)	S_{BET} ($m^2\,g^{-1}$)
Ni–Co–B (1 : 1 : 0)	$Ni_{41.4}Co_{42.4}B_{16.2}$	$Ni_{28.6}Co_{38.6}B_{32.8}$	8.6
Ni–Co–W–B1 (1 : 1 : 0.05)	$Ni_{44.8}Co_{43.9}W_{1.3}B_{10.0}$	$Ni_{23.7}Co_{28.3}W_{1.9}B_{46.0}$	30.2
Ni–Co–W–B2 (1 : 1 : 0.15)	$Ni_{41.1}Co_{43.1}W_{2.7}B_{13.1}$	$Ni_{28.2}Co_{33.1}W_{3.1}B_{35.6}$	33.7
Ni–Co–W–B3 (1 : 1 : 0.30)	$Ni_{40.5}Co_{42.6}W_{4.0}B_{12.9}$	$Ni_{21.4}Co_{34.0}W_{4.5}B_{40.1}$	13.7

[a] Alloy preparation temperature 0 °C.

tachi H600 electron microscope. The amorphous character of the as-prepared alloys was verified by X-ray diffraction (XRD) executed on a Rigaku-rA powder diffractometer with Cu Kα radiation (40 kV, 60 mA). The crystallization process was followed by differential scanning calorimetry (DSC) under N_2 (purity 99.999%) atmosphere with a heating rate of 10 °C min^{-1}. H_2 chemisorption was carried out using a pulsed method [5] at room temperature. Before the measurements, all the samples were treated *in situ* in an Ar flow of 40 ml min^{-1} at 120 °C for 2 h to remove ethanol or other volatile contaminants. Turnover frequencies (TOF) were derived from the amount of H_2 adsorbed and the benzene molecules converted on the samples. The surface electronic states of the alloys were detected by X-ray photoelectron spectroscopy (XPS) performed on a Perkin–Elmer PHI 5000C ESCA system with Al Kα radiation ($h\nu = 1486.6$ eV) at a base pressure of 1.0×10^{-9} Torr. The samples with ethanol were pressed into 1 mm × 13 mm discs and degassed in the pretreatment chamber for 2.0 h at 373 K before being transferred into the analyzing chamber for XPS study. All binding energy (BE) values were referenced to that of contaminant carbon (C 1s = 284.6 eV) [6].

2.3. Activity test

The hydrogenation reaction was carried out in a 500 ml stainless-steel autoclave containing 1.0 g of catalyst, 75 ml of benzene and 75 ml of 99.5% ethanol. The autoclave was purged with hydrogen for several times to exclude air. When the desired reaction temperature was reached, the H_2 pressure was adjusted to 4.0 MPa and the stirring (750 rpm) was commenced, which was taken as the beginning of the reaction. We found that at this stirring rate, the diffusion effect can be readily excluded. The reaction process was monitored by taking small amounts of reaction mixture at intervals, followed by gas phase chromatographic analysis.

3. Results and discussion

3.1. Catalyst characterization

Table 1 lists the surface areas, bulk and surface compositions of the as-prepared alloys. From the bulk composition it can be concluded that the molar ratio of Ni to Co in the bulk is always around 1, consistent with the ratio in the initial solution. The content of tungsten in the alloys increases from 1.3 to 4.0% with the increment of Na_2WO_4 in the solution from 2.5 to 15% with respect to the amount of (Ni + Co), while most of it remains unreduced in the solution. The surface composition is obtained by fitting the XPS spectra of the corresponding elements in the alloys by considering their sensitivity factors [6]. In the fitting, a Guassian–Lorentzian lineshape is employed assuming a linear background. In sharp contrast to the bulk composition, for all four alloys the surface is highly boron-rich, which is consistent with the chemically reduced ultrafine Ni–B for which the bulk composition is $Ni_{71.9}B_{28.1}$ (mol%) while the surface composition is $Ni_{42.4}B_{57.6}$ (mol%) [7]. Meanwhile the surface content of tungsten also increases a little bit from the bulk to the surface.

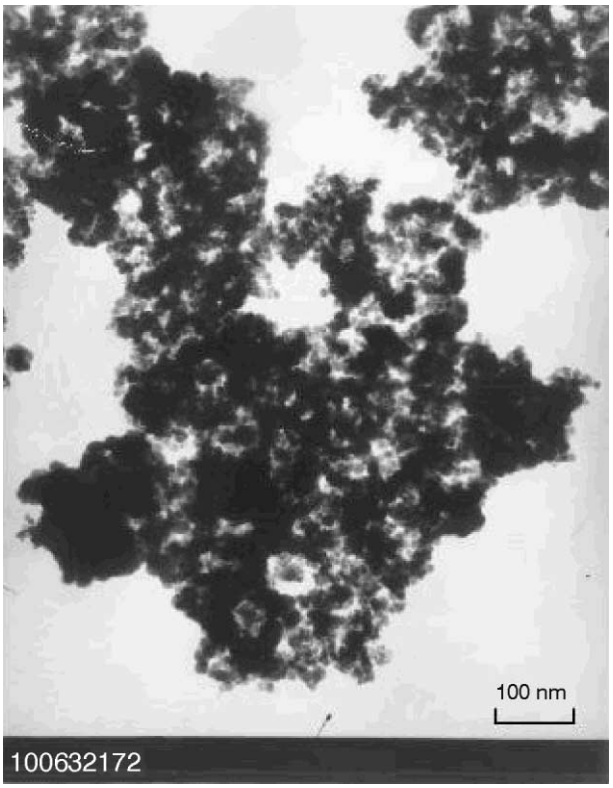

Figure 1. A typical TEM picture of the Ni–Co–W–B alloy.

As compared to Ni–Co–B, alloys with tungsten have larger specific surface area, as shown in table 1. For Ni–Co–B, its specific surface area is only 8.6 $m^2\,g^{-1}$. When 1.3 mol% of W exists in the bulk, the surface area is 30.2 $m^2\,g^{-1}$. The maximum surface area occurs at Ni–Co–W–B2 and drops at higher tungsten content. At the

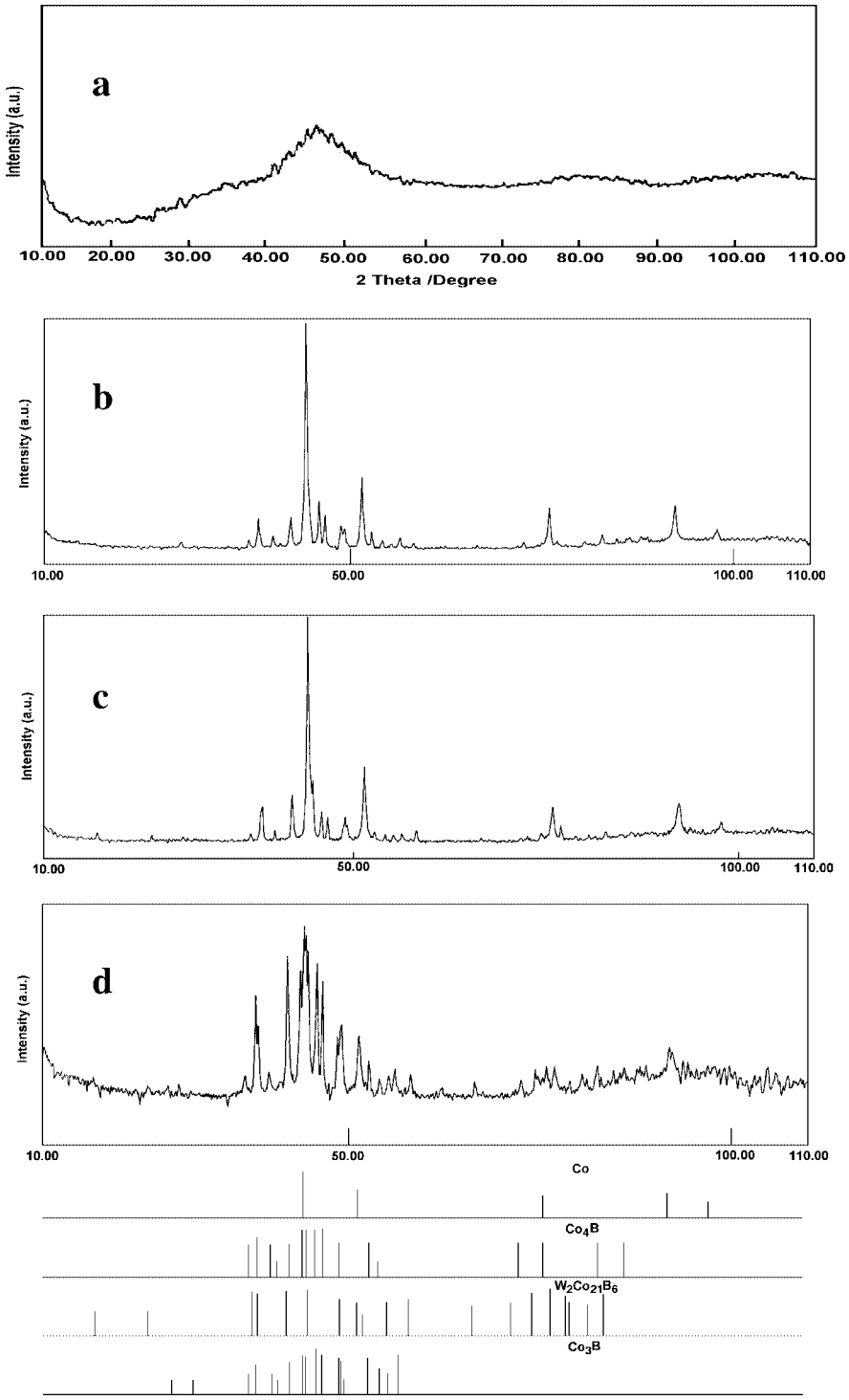

Figure 2. XRD profiles of (a) a typical as-prepared Ni–Co–W–B alloy, (b)–(d) Ni–Co–W–B1, Ni–Co–W–B2 and Ni–Co–W–B3 alloys treated in high-purity N_2 flow at 600 °C for 1 h, respectively.

time being, we are not very sure about the exact mechanism underlying the evolution of the surface area, however, the change of the acidity in the initial solution by adding of basic Na_2WO_4 may be an important factor.

Figure 1 shows the typical TEM morphology for the Ni–Co–W–B alloys. The alloy is mainly composed of particles of ∼20 nm diameter which further agglomerate due to their extremely high surface energy. The amorphous character of the as-prepared alloys is confirmed by XRD patterns in which there is only a broad feature at around $2\theta = 45°$ (figure 2(a)) [8]. After being heated at 600 °C in N_2 flow for 1.0 h, the alloys were crystallized and sharp lines emerged. Due to the multi-component nature of the alloys and the similar atomic radius of Ni and Co tending to form isomorphous substitution, an accurate ascription of these features is quite difficult. However, generally speaking, with the in-

crement of tungsten content in the alloys, the crystallized features became more and more complex. Besides the crystalline phases of Co/Ni, $(Co/Ni)_3B$ and $(Co/Ni)_4B$, the crystalline phase which is attributable to $W_2(Co/Ni)_{21}B_6$ [9] became obvious at higher tungsten content. It is noted that the lines relating to Ni or Co crystalline phase decrease in intensity from Ni–Co–W–B1 to Ni–Co–W–B3, suggesting that tungsten impedes phase separation during crystallization. In other words, it renders better alloying among metals and metalloid.

The crystallization process of the as-prepared alloys was further followed by DSC, as shown in figure 3. For Ni–Co–B amorphous alloy, there are at least five exothermic peaks in the temperature range of 20–600 °C with three main peaks at 156, 286 and 435 °C and two smaller ones at 460 and 502 °C, indicative of the complexity of the crystallization process. With the addition of tungsten, the sharp peak at 286 °C is diminished, while the peak at 156 °C is broadened and shifts to higher temperature. It is worth noting that for the most reactive Ni–Co–W–B2 alloy, besides a broad feature at ∼175 °C, there is only a strong but sharp peak at 429 °C. On the other hand, there are two successive transformation steps for Ni–Co–W–B1 at about 403 and 425 °C and three steps for Ni–Co–W–B3 at about 418, 444 and 463 °C. The DSC profiles clearly demonstrate the change of the microstructure upon tungsten addition. Furthermore, the microstructure in amorphous Ni–Co–W–B2 alloy seems more homogeneous than in other alloys.

The XPS spectra of all four amorphous alloys are illustrated in figure 4. Ni is mainly in its elemental state with Ni $2p_{3/2}$ at 852.6 eV. The small feature at around 856.6 eV is

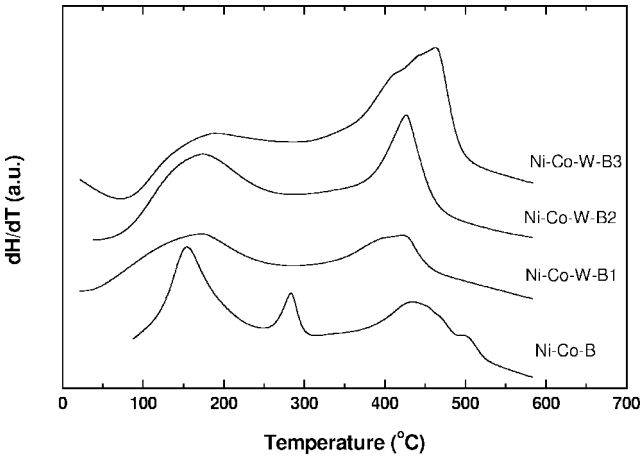

Figure 3. DSC curves of the as-prepared Ni–Co–W–B alloys.

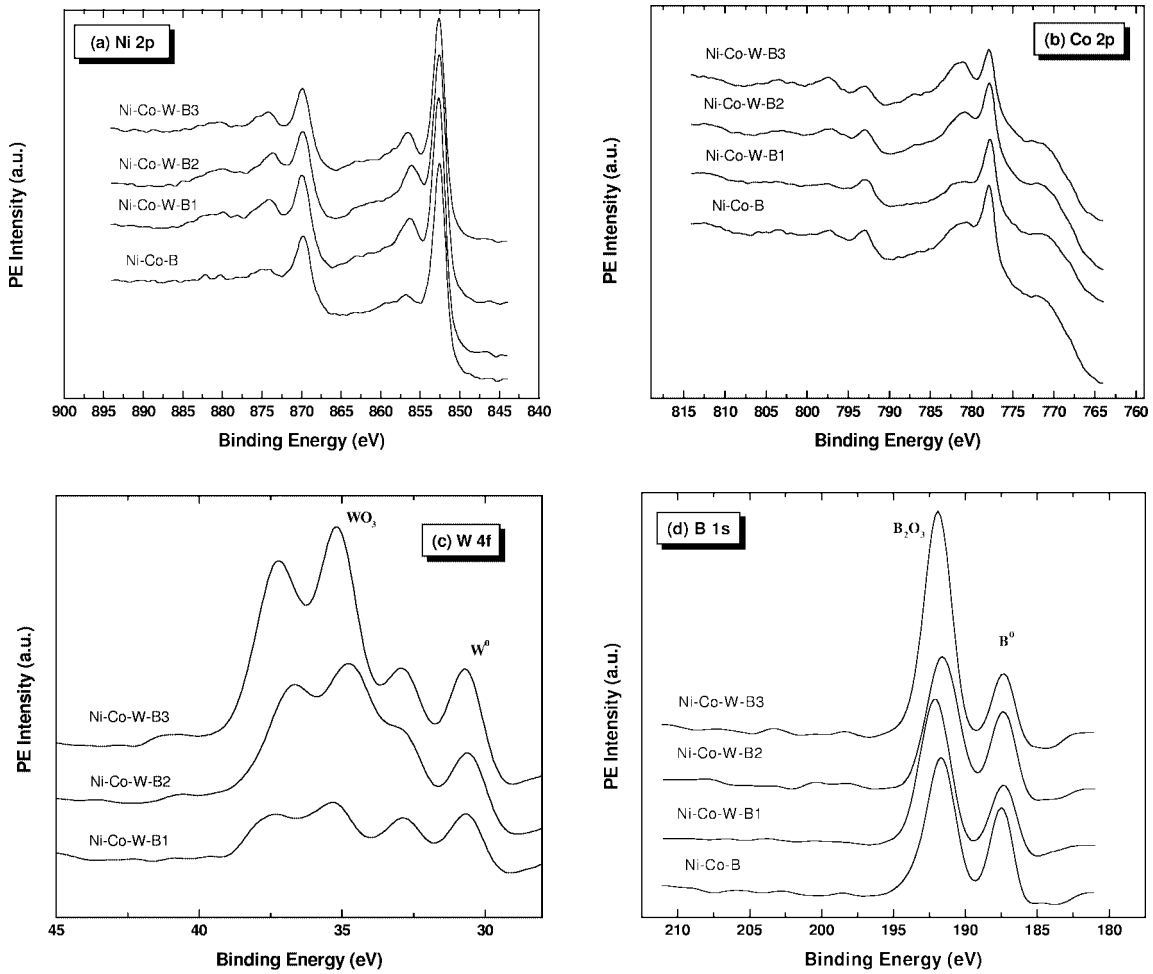

Figure 4. The (a) Ni 2p, (b) Co 2p, (c) W 4f and (d) B 1s XPS spectra of the as-prepared Ni–Co–W–B alloys.

attributed to oxidized nickel [10,11]. Similarly, in all four alloys Co is in the elemental and oxidized state, with Co $2p_{3/2}$ at around 777.8 and 780.9 eV, respectively. It is observed that with the increment of Na_2WO_4 in the solution, the features for oxidized Ni and Co became stronger. It is possible that the basic Na_2WO_4 led to the formation of hydroxides of nickel and cobalt which are less reducible than the metal ions. For B and W, besides their elemental states, B_2O_3 and WO_3 were identified to be the dominant species, which are suggested to be formed during the reduction process [12,13]. It is generally acknowledged that when using borohydride or hypophosphite as reducing agent, three independent reactions will occur: the hydrolysis of the reducing agent, the reduction of the metal ion, and the reduction of the metalloid [13,14]. Chen found that when preparing Fe–B, about 50% of KBH_4 were hydrolyzed to boron oxide, which is inevitable for the reaction carried out in aqueous solution [13].

Previous studies on the chemical states of amorphous Ni–B alloy revealed that elemental boron in Ni–B is positively charged, with its B 1s binding energy shifts from 187.0 eV for pure boron to 188.0 eV. The resulting different electron density on nickel affects the catalytic behavior [15]. In the present case, the B 1s peak for elemental boron is always at ∼187.4 eV, which implies that less electron is transferred from boron to nickel as compared to that in Ni–B.

On the other hand, it is worth noting that in Ni–Co–W–B series alloys tungsten can exist in the elemental state. In a separate experiment (not shown) we found that when there were Na_2WO_4 and $Ni(CH_3COO)_2$ in the solution, WO_4^{2-} can be reduced to elemental W by KBH_4. When the solution contains Na_2WO_4 and $Co(CH_3COO)_2$ or only Na_2WO_4, addition of KBH_4 did not lead to elemental W at all. Such a phenomenon implies that the existence of Ni can induce the reduction of W, or some alloying structure may have formed between Ni and W, which is essential for the improvement of the catalytic activity, as inferred by the superior benzene hydrogenation activity of Ni–Co–W–B series alloys to that of Ni–Co–B shown below.

3.2. Activity in benzene hydrogenation

Figure 5 illustrates the benzene hydrogenation activities of Ni–Co–W–B alloys with different tungsten content with ethanol as the solvent. According to figure 5, the sequence of TOF is Ni–Co–W–B2 > Ni–Co–W–B3 > Ni–Co–W–B1 > Ni–Co–B. As the electron donation property of boron in all four amorphous alloys is identical (figure 4), the microstructures of the alloys should play their own role in determining the difference of the catalytic activity. From XRD and DSC above, we hypothesize that the addition of a certain amount of tungsten can result in a kind of microstructure more appropriate for benzene hydrogenation than that in Ni–Co–B. The sharp high-temperature exothermic peak for Ni–Co–W–B2 in figure 3 may reflect the relatively high population of such structure in the alloy. However, due to the complexity of the quaternary system, a more detailed interpretation on these amorphous alloys cannot be achieved by resolving EXAFS spectra, as there are too many unknown parameters involved.

The influences of preparation temperature and solvents used in the hydrogenation reaction on the performance of Ni–Co–W–B2 alloy were also investigated. For preparation temperatures as low as −15 to 60 °C, no appreciable activity difference can be observed, while solvent can greatly influence the hydrogenation behavior. It is interesting that when alcohols were used as solvents, the chain length closely correlates to the hydrogenation activity of Ni–Co–W–B2. Table 2 shows that the H_2 uptake rate increases with the length of carbon chain. The order of rate is *n*-butanol > ethanol > methanol, which can be rationalized by the argument that a hydroxyl group competitively adsorbs on or blocks the active site of the catalyst. When using alkanes as solvents, the catalyst can be four times as reactive as when using methanol. Thus cyclohexane, the product, can be used as solvent, which simplifies the separation procedure in liquid phase reaction. The influence of solvents on the activity of

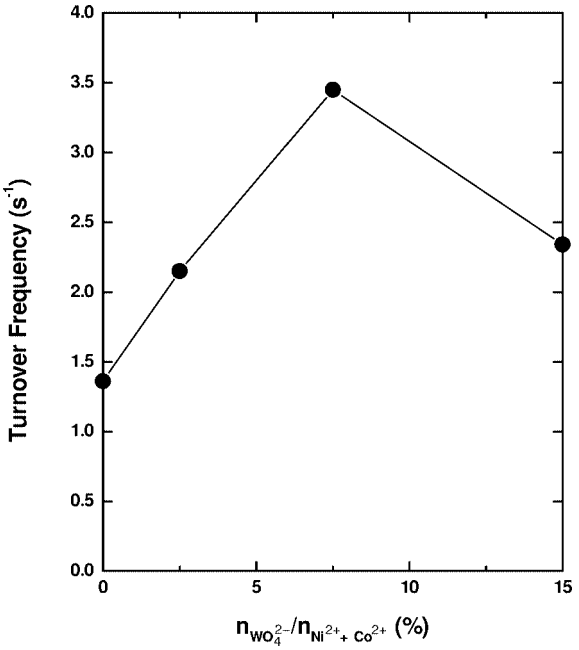

Figure 4. The relationship between benzene turnover frequencies and the content of Na_2WO_4 in the initial solution. Reaction conditions: catalyst 1.0 g, benzene 75 ml, ethanol 75 ml, P_{H_2} 4.0 MPa, temperature 100 °C, stirring rate 750 rpm. Alloy preparation temperature 0 °C.

Table 2
The influence of solvent on the catalytic activity of Ni–Co–W–B2 alloy.[a]

Solvent	H_2 uptake rate (mmol s^{-1} g_{cat}^{-1})
Methanol	0.19
Ethanol	0.22
n-butanol	0.37
Isopentane	0.86
Cyclohexane	0.85

[a] Reaction conditions: catalyst 1.0 g, benzene 75 ml, solvent 75 ml, P_{H_2} 4.0 MPa, temperature 100 °C, stirring rate 750 rpm. Alloy preparation temperature 0 °C.

Table 3
Surface chemical composition of the fresh and the partially deactivated Ni–Co–W–B2 amorphous alloy.

Ni–Co–W–B2	Surface atomic density (%)							
	Ni^0	Ni^{2+}	Co^0	Co^{2+}	B^0	B^{3+}	W^0	W^{6+}
Fresh	19.5	8.7	21.9	11.2	13.8	21.8	1.1	2.0
Partially deactivated[a]	13.3	14.9	10.1	23.1	5.7	30.0	0.7	2.2

[a] After 30 runs of benzene hydrogenation.

Ni-based catalyst is not unexpected. On Ni single crystals methanol is dissociatively adsorbed [16], while for cyclohexane a detailed ARUPS study [17] revealed that the electronic structure of cyclohexane on Ni(111) is virtually unchanged as compared to the gas phase spectrum, implying the weak van der Waals interaction between cyclohexane and Ni(111). A similar trend is supposed to be held by these solvents on the Ni–Co–W–B2 alloy.

We noticed that for the Ni–Co–W–B2 alloy after 30 runs of hydrogenation under the conditions illustrated in figure 5, the activity dropped to about 50% of that of the first run. While XRD always gave a broad feature at around $2\theta = 45^\circ$ and BET did not show considerable difference, XPS revealed substantial oxidation of the amorphous alloy. The surface atomic compositions of the fresh and the partially deactivated catalysts are calculated and listed in table 3. It is found that oxidation occurred for all four elements in the alloy. The oxidation is supposed to be the high reactivity of nanoparticles to residual oxygen in the reaction system, as we previously reported for the deactivation of an amorphous Ni–B/SiO_2 catalyst in selective hydrogenation of cyclopentadiene [18].

4. Conclusion

Quaternary ultrafine Ni–Co–W–B amorphous alloys prepared by a chemical reduction method exhibit excellent activity in benzene hydrogenation to cyclohexane. It is found that the introduction of a certain amount of tungsten can substantially promote their catalytic activities. As there is no measurable electronic effect, tungsten is supposed to tailor the microstructure of the Ni–Co–B amorphous alloy, leading to active centers more appropriate for benzene hydrogenation to cyclohexane.

Acknowledgement

This work is supported by the Special Foundation for Doctor Candidate of the State Education Commission of PR China, the National Natural Sciences Foundation of China and SINOPEC.

References

[1] A. Stanislaus and B.H. Cooper, Catal. Rev. Sci. Eng. 36 (1994) 75.
[2] T. Katona and A. Molnar, J. Catal. 153 (1995) 333;
K. Hashimoto, Mater. Sci. Eng. A 226 (1997) 891;
J.F. Deng, H.X. Li and W.J. Wang, Catal. Today 51 (1999) 113.
[3] M. Shibata and T. Masumoto, Prep. Catal. 4 (1987) 353;
A. Molnar, G.V. Smith and M. Bartok, Adv. Catal. 36 (1989) 329.
[4] H. Yamashida, M. Yoshikawa, T. Funabiki and S. Yoshida, J. Chem. Soc. Faraday Trans. I 82 (1986) 1771;
H. Yamashida, T. Kaminade, T. Funabiki and S. Yoshida, J. Mater. Sci. Lett. 4 (1985) 1241;
M. Shibada and T. Masumoto, Stud. Surf. Sci. Catal. 31 (1987) 353;
J.A. Schreifels, P.L. Maybury and W.E. Swartz, J. Catal. 65 (1980) 195;
H. Yamashida, T. Funabiki and S. Toshida, J. Chem. Soc. Chem. Commun. (1984) 868.
[5] P.I. Lee and J.A. Schwarz, J. Catal. 73 (1982) 272.
[6] *Handbook of X-ray Photoelectron Spectroscopy* (Perkin–Elmer, Eden Prairie, MN, 1992).
[7] J.F. Deng, J. Yang, S.S. Sheng, H.R. Chen and G.X. Xiong, J. Catal. 150 (1994) 434.
[8] J. Wonterghem, S. Mørup, S.W. Charles and S. Wells, Nature 322 (1986) 622.
[9] *PDFMaint Version 3.0, Powder Diffraction Database* (Bruker Analytical X-ray Systems GmbH, 1997).
[10] M.S. McIntyre and M.G. Cook, Anal. Chem. 47 (1975) 2208.
[11] H. Windawi and C.D. Wagner, in: *Applied Electron Spectroscopy for Chemical Analysis*, eds. H. Windawi and F. Ho (Wiley, New York, 1982) ch. 9.
[12] V.M. Deshpande, W.R. Patterson and C.S. Narasimhan, J. Catal. 121 (1990) 165.
[13] Y. Chen, Catal. Today 44 (1998) 3.
[14] G.O. Mallory and J.B. Hajdu, eds., *Electroless Plating: Fundamentals and Applications* (American Electroplaters and Surface Finishers Society, 1990).
[15] Y. Okamoto, Y. Nitta, T. Imanaka and S. Teranishi, J. Chem. Soc. Faraday Trans. I 15 (1979) 2027;
Y. Okamoto, Y. Nitta, T. Imanaka and S. Teranishi, J. Catal. 64 (1980) 397.
[16] H. Yang, J.L. Whitten and C.M. Friend, Surf. Sci. 313 (1994) 295.
[17] A.K. Myers, G.R. Schoofs and J.B. Benziger, J. Phys. Chem. 91 (1987) 2230.
[18] W.J. Wang, M.H. Qiao, H.X. Li, W.L. Dai and J.F. Deng, Appl. Catal. A 168 (1998) 151.